Journal of Alloys and Compounds 510 (2012) 38–45

Contents lists available at ScienceDirect

Journal of Alloys and Compounds

journal homepage: www.elsevier.com/locate/jallcom

Interface reaction between SnAgCu/SnAgCuCe solders and Cu substrate subjected to thermal cycling and isothermal aging

Liang Zhang[a,b], Song Bai Xue[a,*], Guang Zeng[a], Li Li Gao[a], Huan Ye[a]

[a] College of Materials Science and Technology, Nanjing University of Aeronautics and Astronautics, Nanjing 210016, China
[b] School of Mechanical and Electrical Engineering, Xuzhou Normal University, Xuzhou 221116, China

ARTICLE INFO

Article history:
Received 4 April 2011
Received in revised form 7 August 2011
Accepted 9 August 2011
Available online 30 August 2011

Keywords:
Rare earth
Intermetallic compound
Growth kinetics
Thermal cycling

ABSTRACT

Trace amount of rare earth Ce (0.03 wt.%) was added into SnAgCu solder in order to reform the properties of the solder. In this study, interface reaction mechanism during thermal cycling and isothermal aging, was studied by studying the formation and growth of the intermetallic compound (IMC) at the solder (SnAgCu or SnAgCuCe)/Cu interface, and the growth kinetics which forming IMC in both systems (SnAgCu or SnAgCuCe) were also investigated under different aging conditions. The results show that the morphology of IMCs formed both at SnAgCu/Cu and SnAgCuCe/Cu interfaces was gradually changed from scallop-like to planar-like, and the thickness of different IMCs evolved with the increasing of aging time. The results also indicate that the growth rate of IMC at both interfaces during thermal cycling was higher than that during isothermal aging. Especially, the addition of amount of rare earth Ce into the SnAgCu solder can refine the microstructures; decrease the thickness of the intermetallic compound layer of SnAgCu solder alloys.

1. Introduction

SnPb alloys have long been considered as the most popular materials for soldering the electronic components and devices because of their unique combination of material properties and low cost [1,2]. However, emerging environmental regulations world wide, most notably in Europe and Japan, have targeted the elimination of Pb usage in electronic assemblies due to the inherent toxicity of Pb [3]. Owing to the realization of the harmful influence of lead and lead containing alloys on the environment and human health, many Pb-free solder-alloys have been developed to replace SnPb solders in electronic applications [4]. Among several candidate alloys, the SnAgCu solder (SAC) family is believed to be the most promising. SnAgCu solder has been proposed as the most promising substitute for lead-containing solders because of its relatively low melting temperature, its superior mechanical properties, and its relatively good wettability, thus the SnAgCu solders are extensively used as solder materials in the electronic industry [5–7]. The ternary-eutectic composition is now thought to be close to Sn3.5Ag0.9Cu with a melting point of 217 °C. The main benefits of this alloy system are its relatively low melting temperature compared with SnAg binary eutectic alloy and its generally superior mechanical properties, as well as relatively good solderability [8,9]. Thus, SnAgCu alloys have been proposed by the Japanese (Sn3.0 wt.%Ag0.5 wt.%Cu), the EU (Sn3.8 wt.%Ag0.7 wt.%Cu) and the US (Sn3.9 wt.%Ag0.6 wt.%Cu) consortiums as replacements for conventional SnPb eutectic solder [10]. But the microstructures of these alloys were coarse and in order to refine it, Ge [11], Bi [12], Fe [13], Mn [14], Co [15], Zn [16], Ga [17], In [18], B [19], Sb [20], and Ni [21] elements were used to investigate the effect on the microstructure. Recently, trace rare earth (RE) elements [22–24] were also added into lead-free solder alloys to form better solder alloys. With the addition of RE, the properties such as microstructure, mechanical and wetting behavior of SnAgCu [25,26] were all improved. However, there are still some problems to be resolved for SnAgCu solders, such as the argument about the best composition, still its high soldering temperature, large undercooling and, in particular, the formation of large brittle intermetallic compounds (IMCs) as primary precipitates which may lead to serious problems under stressed conditions in the actual service for printed wiring boards.

Cu is extensively used as the contact metallization in conventional electronics assemblies particularly on printed circuit boards (PCBs) and increasingly as the interconnection layer on semiconductor devices in electronics industry, while Sn-based alloys are universally used as interconnection materials [27–29]. The resulting Cu–Sn intermetallic compounds formed during soldering process show an important role in the wettability of solders [30]. However, reliability concerns arise when it is used together with high Sn content solders due to rapid consumption of Cu and spallation of Cu–Sn IMCs [31–35]. During reflow of the Cu/SnAgCu

* Corresponding author. Tel.: +86 25 8489 6070; fax: +86 25 5211 2626.
E-mail address: yeehone@126.com (S.B. Xue).

0925-8388/$ – see front matter.
doi:10.1016/j.jallcom.2011.08.044

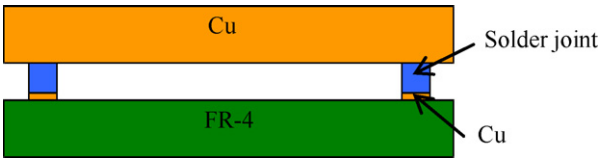

Fig. 1. Schematic cross-sectional geometry of the solder/Cu samples.

joint system, Cu_6Sn_5 forms first at the interface. Cu_3Sn will form later between Cu and Cu_6Sn_5 by solid-state reaction to satisfy the requirements of local equilibrium [36]. Tu and Thompson [37] propose that the growth rate of Cu_6Sn_5 in bimetallic Cu–Sn thin film is linear and the reduction rate of Cu_6Sn_5 due to the growth of Cu_3Sn is parabolic. Formation of the intermetallic compound (IMC) layers at the interface is an indication of good bonding between solder and the metal pad. However, excessive intermetallic growth and the brittle nature of the intermetallic layer can be detrimental to the mechanical reliability of the joint [38]. Moreover recent investigations [39–41] had reported that the growth of Cu–Sn IMC layer had a degraded effect on the solder joint reliability, with increasing thickness of the Cu–Sn IMC layer, the thermal fatigue life, tensile strength and fracture toughness of solder joints will decrease. As a result, the interfacial reaction may be directly related to the solder joint reliability in the electronic package. In this sense the interfacial behavior needs to be investigated more systematically from the soldering stage to the serve condition of thermal cycling and isothermal aging, especially for new SnAgCu–X (X = RE, Bi, Ni, etc.) solders.

Two lead-free solders, $Sn_{3.8}Ag_{0.7}Cu$ and $Sn_{3.8}Ag_{0.7}Cu_{0.03}Ce$, had been used in this work. These two solders were selected because the former one is recommended as the best candidate for SnPb solders [42] and the latter one exhibits outstanding wettability and mechanical properties [43]. This paper begins by presenting results for the interfacial reaction between SnAgCu/SnAgCuCe solders and Cu substrates.

2. Experimental

2.1. Preparation of samples

The pure Sn (99.99%), Sn–Cu alloy (415 °C), Sn–Ag alloy (480 °C) and Cu–Ce alloy (424 °C) were used as raw materials. The raw materials of Sn, Sn–Cu alloy, Sn–Ag alloy, Cu–Ce alloy were melted in a ceramic crucible, and melted at 550 °C ± 1 °C for 40 min. To homogenize the solder alloy, mechanical stirring was performed every 10 min using a glass rod. During the melting, KCl + LiCl (1.3:1), were used over the surface of liquid solder to prevent oxidation. The molten alloys were chill cast ingots in a copper mold. Then they were solidified by nominally air-cooling. All solder specimens were heat treated at 125 °C for an hour to stabilize the microstructure of the solder alloys. The sandwich specimens (Fig. 1) were prepared by joining Cu substrate and FR-4 (Flame Retardant Type 4) substrate with SnAgCu/SnAgCuCe solders through a full air convection oven, the structure leads to a high thermal stress–strain cycling in the soldered joints during thermal cycling due to mismatch of thermal expansion coefficient between copper and FR-4 (Flame Retardant Type 4). Samples to be cross sectioned were embedded in epoxy resin. They were ground with 320, 600 and 1200 grade abrasive sandpapers, and then polished with 6 μm, 3 μm, and 1 μm diamond suspensions. In order to reveal details of the interfacial structure, 0.04 μm alumina and 0.025 μm colloidal silica suspensions were used for final polishing.

2.2. Thermal cycling and isothermal aging

Thermal cycling and isothermal aging were used for solid-state IMC growth investigations. The samples were subjected to a cycling temperature reliability test in a three-zone furnace chamber, which follows the JEDEC standard temperature range of −55 to +125 °C with a cycle time of 56 min. The ramp rate was about 12 °C/min^{-1} and the dwell time was 12 min at each temperature extreme. Test specimens were extracted out every 100 cycles to investigate the morphological and interfacial behavior of the solder joint. The exposure time at 125 °C is equal to the total dwell time spent at the high-temperature soak period for the thermal cycling profiles. This is compared to the isothermal aging results at 125 °C.

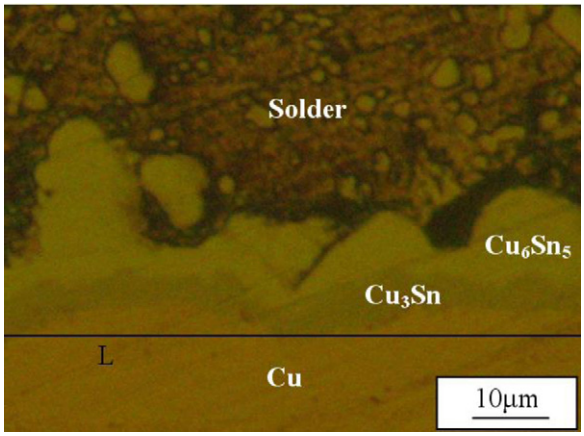

Fig. 2. Illustration of the interfaces between the different layers for the SnAgCu sample stored at 125 °C for 2000 h.

2.3. Identification and thickness measurement of IMCs

A Quanta200 scanning electron microscope (SEM) equipped with a thermo-electron X-ray energy dispersion spectrometry (EDS) was used to examine the microstructure and determine the phases in the interfacial region. To observe clearly the morphology of IMC at the interface, the solder matrix was etched away using a $5HNO_3 + 95CH_3OH$ solution for several seconds. Considering the irregular shape of the Cu_6Sn_5 and Cu_3Sn layers as shown in Fig. 2, their thicknesses were digitally measured by using the software "Image J". While, the average thickness of the IMC layers (x) in liquid aged solder joints were calculated through dividing the integrated area (A) by the length of the IMC layers (L), as shown in the following equation:

$$x = \frac{A}{L} \quad (1)$$

3. Results and discussion

3.1. Interfacial microstructure

SEM micrographs of a same magnification of the solders/Cu interface after thermal cycling and isothermal aging are presented in Figs. 3–6.

Fig. 3 shows SEM micrographs between SnAgCu solder and bare Cu substrates of reaction couples aged at 125 °C for different aging times. These figures show the accelerated growth of the intermetallic compound layer with the aging time during isothermal aging. Binary intermetallic compound layers were formed at the solder joints on copper substrate. The results show that the morphology of IMCs formed both at SnAgCu/Cu and SnAgCuCe/Cu interfaces gradually changed from scallop-like to planar-like, and different IMC thickness developed with increasing aging time. The intermetallic layer appears to be comprised of two compounds of different compositions. As an EPMA analysis results, the planar intermetallic layer next to the solder possesses a compositions (at.%) of Cu:Sn = 6.1:5, which corresponds to the Cu_6Sn_5 phase. The compositions of the intermetallic layer next to the copper is Cu:Sn = 3:1, which corresponds to the Cu_3Sn phase. The compound on the copper side of the interface primarily contains copper, while the compound on the solder side of the interface is particularly rich in copper and poor in silver. After soldering, the Cu_6Sn_5 IMC located at the solder/Cu interface was identified by means of EDS analysis and the thickness of the intermetallics was approximately 3.5 μm, but Cu_3Sn IMC was not found as shown in Fig. 3(a). However, the Cu_3Sn layer exists at all time periods for the aging temperature of 125 °C. As shown in Fig. 3(b)–(d), the Cu_6Sn_5 intermetallic layer was the dominant phase. These findings support previous research on this system by Yoon and Jung [44]. They investigated the intermetallic compound (IMC) growth during solid-state isothermal aging for $Sn_{3.5}Ag_{0.7}Cu$ solder on Cu substrate. They found that the

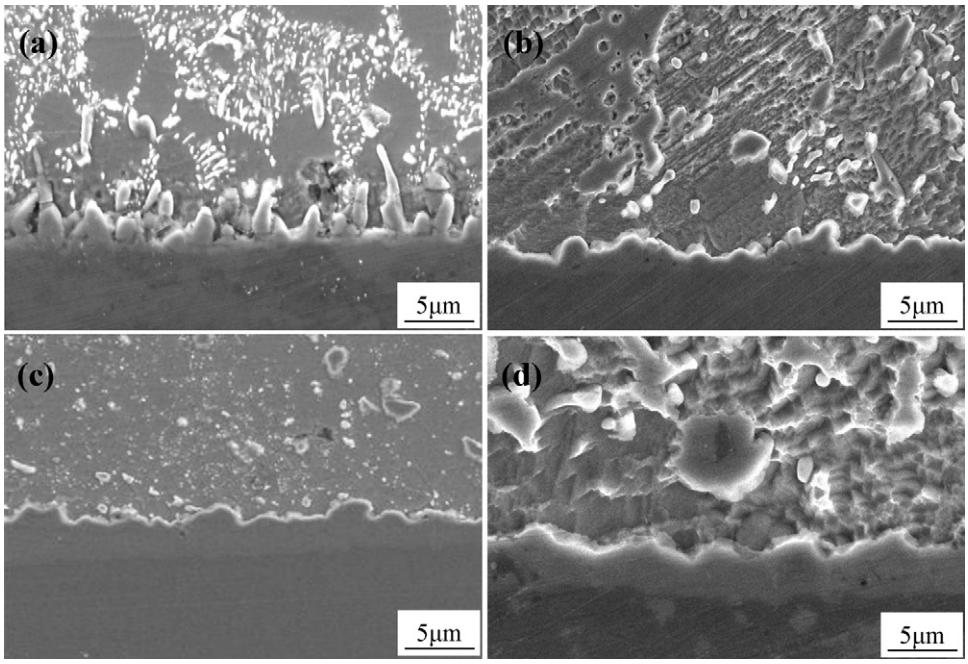

Fig. 3. Evolution of interfacial structure with aging time for SnAgCu solder: (a) after soldering, (b) 300 h, (c) 600 h, and (d) 900 h.

intermetallic compounds interface exhibited a duplex structure of Cu_6Sn_5 and Cu_3Sn intermetallics. The similar results were found for SnAgCuCe solder on Cu substrate as shown in Fig. 4. This observation indicated that the rare earth Ce had significant influence on the formation and initial thickness of the IMC layer during soldering. Thus, after subjected to isothermal aging for 300 h, 600 h and 900 h, the interfacial IMC layer of the monolithic SnAgCu solder joint was observed to grow more obviously than that of the SnAgCuCe solder joints. Ahat et al. demonstrated that the strength of solder joint decreased with increasing thickness of the IMC layer [45,46].

Thermal cycling or thermo-mechanical fatigue testing of solder joints is very important as far as the reliability of the solder joint is concerned. Because of large difference in the coefficient of thermal expansion (CTE) of the different constituents in the packaged assembly, stresses and strains vary with temperature leading to cyclic strain or inelastic energy damage and fatigue failure of the solder joints [47]. From the morphological studies of the as-reflowed and thermally cycled samples, the IMC layers should grow with the number of temperature cycles. Cross-sectional morphologies of the interfacial Cu–Sn intermetallic layers in SnAgCu/SnAgCuCe solder joint during thermal cycling process

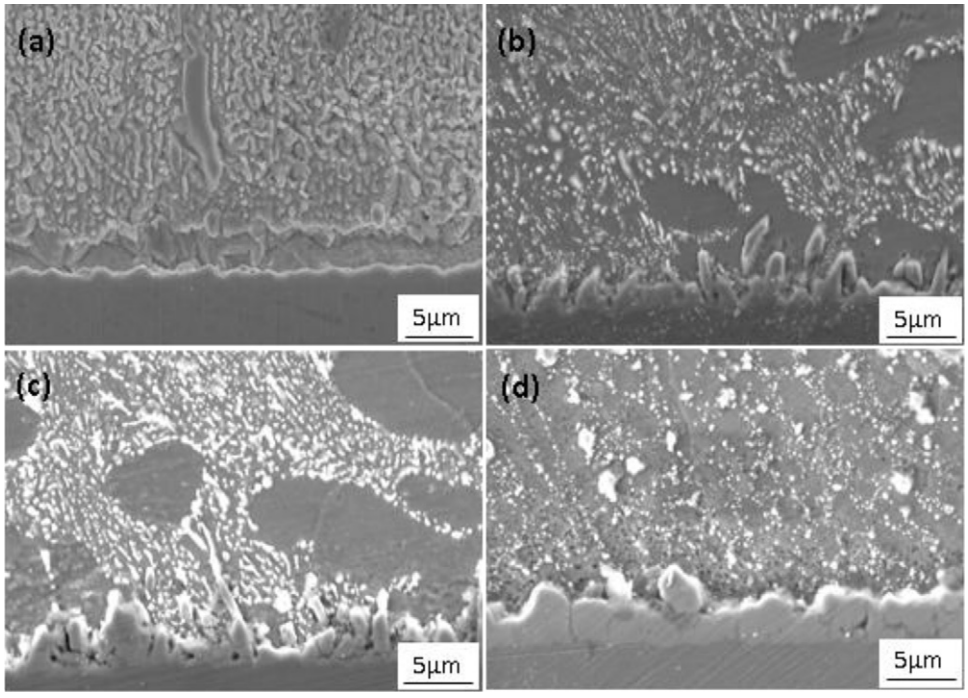

Fig. 4. Evolution of interfacial structure with aging time for SnAgCuCe solder: (a) after soldering, (b) 300 h, (c) 600 h, and (d) 900 h.

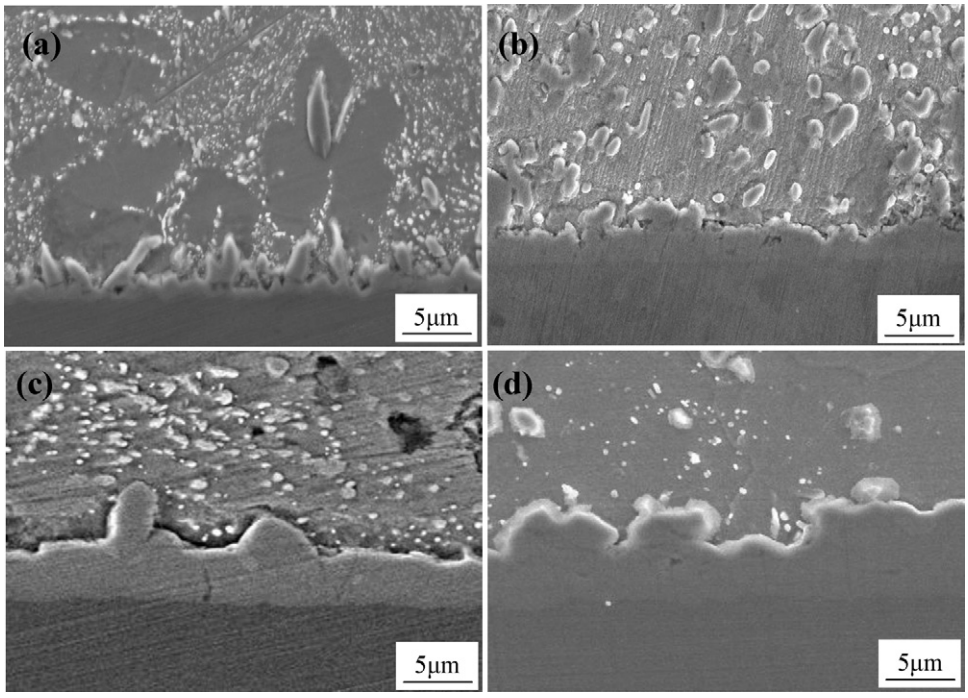

Fig. 5. Evolution of interfacial structure with thermal cycling aging time for SnAgCu solder: (a) after soldering, (b) 300 cycles, (c) 600 cycles, and (d) 900 cycles.

aging for 0, 300, 600 and 900 cycles during −55 °C to 125 °C are shown in the series of SEM micrographs in Figs. 5 and 6. The interfacial Cu–Sn intermetallic layers are located, with only the Cu_6Sn_5 found in as-solidified sample while both the Cu_6Sn_5 and the Cu_3Sn are found in all thermal cycled samples. The formation of Cu_6Sn_5 intermetallic layers in solder joint during the reflow process arises by interfacial reactions between its constituting species, Sn from the solder and Cu from the copper land pad. Since the morphological change of Cu_6Sn_5 must have started from scallops, the top surface of the Cu_6Sn_5 layer remained somewhat wavy. During isothermal aging, the Cu_6Sn_5 in the layer grows by inter-diffusion of Cu and Sn and reaction with each other, while the Cu_3Sn forms and grow by reactions between the Cu substrate and Cu_6Sn_5 IMC layer. The IMC layers formed in the SnAgCu/Cu samples were thicker than those in the SnAgCuCe/Cu samples for the same thermal aging time. In addition, it is interesting to note that the spalling behavior of intermetallic compounds in SnAgCu/SnAgCuCe solder joints subjected to thermal cycling loading. The spalling phenomenon was caused by (i) interface structure change and (ii) cyclic shear stresses and strains induced during temperature cycling [48].

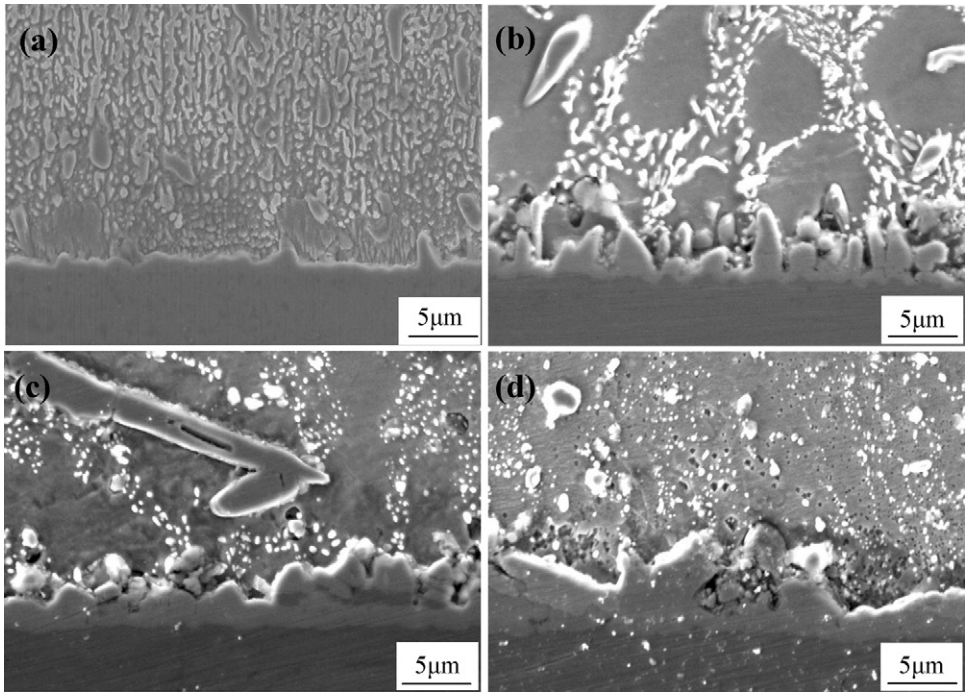

Fig. 6. Evolution of interfacial structure with thermal cycling aging time for SnAgCuCe solderL (a) after soldering, (b) 300 cycles, (c) 600 cycles, and (d) 900 cycles.

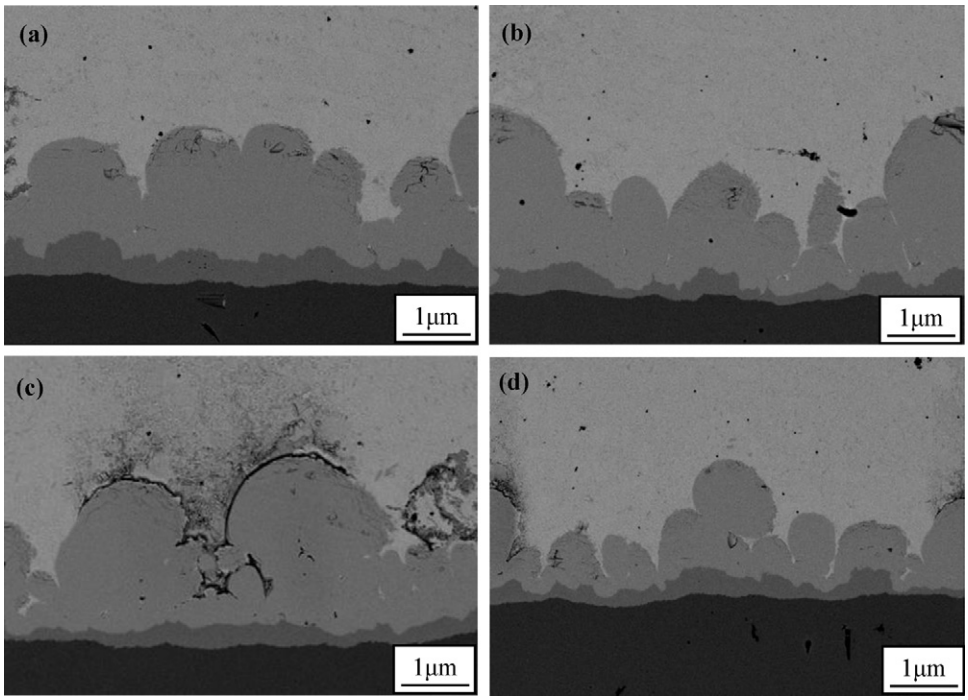

Fig. 7. Cross-sectional micrographs of solder joints: (a) SnAgCu/Cu (thermal cycling: 300 cycle), (b) SnAgCuCe/Cu (thermal cycling: 300 cycles), (c) SnAgCu/Cu (aging: 300 h), and (d) SnAgCuCe/Cu (aging: 300 h).

3.2. IMC thickness and activation energy

Fig. 7 shows the backscatter electron micrographs for the samples with different solders and aging conditions. At this aging time, Cu_6Sn_5 and Cu_3Sn IMCs all can be detected and seen in these figures. In solid-state aging (isothermal aging or thermal cycling aging), the morphology of Cu_6Sn_5 changed from scallop-type to layer-type. This change requires the growth of IMC in the valleys between the scallops. In other words, in the initial stage of the solid-state aging the IMC growth is faster in the valley than at the peak of scallops. Between the Cu_6Sn_5 grains, there are molten solder channels extending all the way to the Cu_3Sn/Cu interface. Since the Cu_3Sn compound layer is so thin, these channels serve as fast diffusion and dissolution paths of Cu in the solder to feed the interfacial reaction.

Fig. 8 shows a schematic diagram of this growth where the arrows show the Cu flux [49]. The arrow (path 1) from the peak of a scallop to the valley is driven by the curvature effect. The arrow (path2) from Cu to the solder is driven by the interfacial reaction between Cu and solder to form the IMC. They combine to form a layer-type Cu_6Sn_5. In solid-state aging, the solubility and diffusivity of Cu in Sn are much less than those in the molten solder; hence, the rate of IMC growth is much slower. This is more so when the IMC layer becomes a diffusion barrier and the growth becomes diffusion controlled by "path 2." Moreover, Chung et al. [50] identified Cu-enriched regions at phase boundaries between Cu_6Sn_5 and Cu_3Sn by high-resolution transmission electron microscopy. Such regions were about 3–6 nm thick due to a large lattice mismatch. Similar Cu-enriched regions were also observed at the grain boundary of Cu_6Sn_5. The existence of these Cu-enriched regions suggests that grain boundary and phase boundary diffusion of Cu atoms were the dominant mechanisms for the growth of Cu_6Sn_5 and Cu_3Sn in the early stages of soldering reactions. Based on above discussions, the effect of rare earth Ce on Cu diffusion can be utilized to interpret the different IMC thickness of SnAgCu/Cu and SnAgCuCe/Cu interface. Considering a Cu/Cu_3Sn/Cu_6Sn_5/solder diffusion couple, one notes that the net diffusion driving force going from Cu to solder is reduced if the Cu concentration in solder increases [51]. Rare earth has high affinity to the constituent of Sn [52], which will result in a decreased driving force for Cu–Sn intermetallic compound formation. Moreover, with a reduced driving force for Cu diffusion, the Cu atomic flux moving from Cu side to the solder side decreases. The decrease of Cu flux to solder can low the reaction percentage ($9Cu + Cu_6Sn_5 \rightarrow 5Cu_3Sn$). Consequently, the addition of Ce into SnAgCu will affect the growth thickness of IMCs.

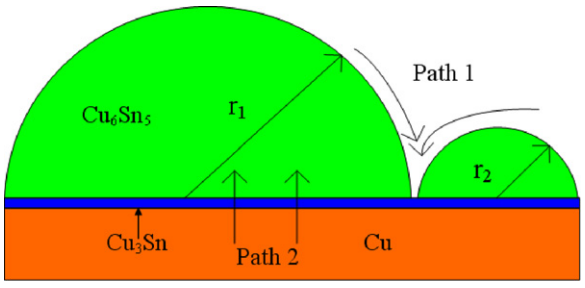

Fig. 8. Schematic diagram of Cu diffusion paths during solid-state aging (isothermal aging or thermal cycling aging).

The average thickness of Cu_3Sn, Cu_6Sn_5, and the total layer of $Cu_3Sn + Cu_6Sn_5$ are plotted in Fig. 8. The standard deviation is 0.03–0.05 μm. For Sn–Cu reaction couple after a few seconds, Cu_3Sn is either absent or too thin to be resolved by scanning electron microscopy. The TEM observations show that the formation of interfacial intermetallic compound Cu_3Sn may occur through a homogeneous nucleation process within the amorphous [53]. Obviously, the increase of total IMC thickness is mainly due to the growth of Cu_3Sn rather than Cu_6Sn_5. The thickness of IMC layer at SnAgCuCe solder/Cu interface is obviously smaller than that at SnAgCu solder/Cu interface, especially for Cu_3Sn layer (Fig. 9).

After the Cu atoms arrive at the interface of Cu_3Sn/Cu_6Sn_5 by diffusion through the grain boundaries of the Cu_3Sn layer, the following interfacial reaction happens:

$$Cu_6Sn_5 + Cu \rightarrow Cu_3Sn \quad (2)$$

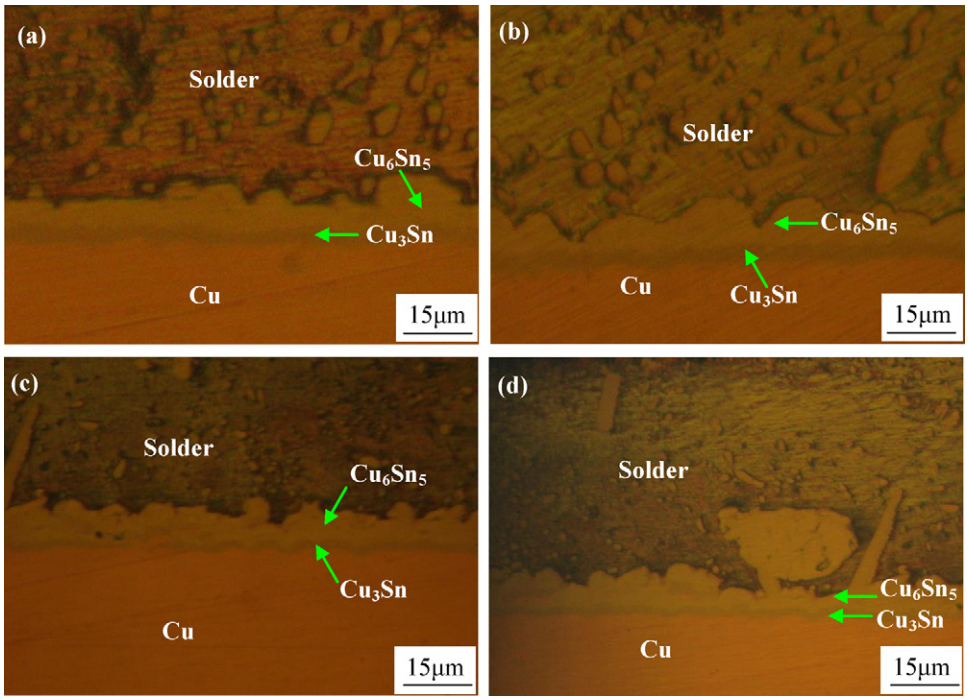

Fig. 9. Cross-sectional micrographs of solder joints: (a) SnAgCu/Cu (thermal cycling: 1200cycle), (b) SnAgCu/CuCe (thermal cycling: 1200 cycles), (c) SnAgCu/Cu (aging: 1200 h), and (d) SnAgCuCe/Cu (aging: 1200 h).

By this reaction, Cu_6Sn_5 is converted to Cu_3Sn at the interface. Because of this reaction, the amount of Cu atoms that can diffuse to the interface of Cu_6Sn_5/solder is greatly reduced. As the result, Cu_3Sn grows rapidly with temperature and time by consuming Cu_6Sn_5 at the interface of Cu_3Sn/Cu_6Sn_5. The growth of Cu_6Sn_5 on the solder side mainly depends on the availability of Cu atoms in the solder. Since most of the Cu atoms in the bulk solder have been taken to form Cu_6Sn_5 particles in the eutectic structure, the amount of free Cu atoms that can diffuse to the solder/Cu_6Sn_5 interface is very small, greatly limiting the growth of Cu_6Sn_5 on the solder side. Therefore, during thermal aging, the Cu_3Sn layer expanded on both sides, resulting in the shifting of the Cu/Cu_3Sn interface towards Cu pad and the Cu_3Sn/Cu_6Sn_5 interface towards the Cu_6Sn_5. That is why Cu_6Sn_5 grew much slower than Cu_3Sn at 125 °C.

The kinetics of IMCs growth can be diffusion controlled or interfacial-reaction controlled [54,55]. The growth kinetic parameters of an IMC layer can be determined by plotting its measured thickness as a function of the exposure time at given temperatures as shown in Fig. 8. For the growth of the IMCs layer, because the diffusion of Cu through Cu_3Sn is the rate-limiting factor, its thickness as a function of the time can be expressed as the following equation [56]:

$$X_t = X_0 + \sqrt{kt} \tag{3}$$

where X_t is the IMC layer thickness at aging time t, X_0 is the initial IMC layer thickness after soldering, and k is the diffusion coefficient as a function of temperature. The IMC layer growth is a diffusion dominant process and so the Arrhenius relationship is applicable. The activation energies for the IMC growth were calculated using the Arrhenius relationship, such that [57]:

$$k = k_0 \cdot \exp\left(\frac{-Q}{RT}\right) \tag{4}$$

where k_0 is the diffusion constant, Q is the activation energy for the growth of the interfacial IMC layer, T is the temperature in Kelvin (K), and R is the gas constant, 8.314 J/mol K.

From the measured thickness data, k can be determined for each experimental temperature. Using Eq. (4), the activation energy Q can be determined from the slope of the straight line obtained by plotting $\ln(k)$ against $1/T$. Eq. (4) could then be expressed as follows, by taking the logarithms of both sides of the equation [58].

$$\ln(k) = \ln(k_0) - \left(\frac{Q}{RT}\right) \tag{5}$$

The activation energies were calculated from the slope of the Arrhenius plot using a linear regression model.

From the point of view of solder joint reliability, the thickness of IMC layer is a concern. Fig. 10 shows the thickness of the IMC layer as a function of the aging time for thermal cycling and isothermal aging. It is found that the mean thickness of the interfacial IMC layer increases linearly with the square root of the aging time and the growth was faster for thermal cycling aging. The atomic diffusion of Cu and Sn through the IMC layer is the main controlling process for the IMC growth during aging [59]. Thus, the transaction times for the Cu_6Sn_5 phase to transform into the Cu_3Sn phase are related to the complete consumption of the Sn phase in the Cu pillar bumps. For both Cu_6Sn_5 and Cu_3Sn, with a small amount of Ce additions, the thickness of IMC layer at solder/Cu joint interface decreased, e.g., about 1 μm, for total IMC layer, about 2 μm during isothermal aging. During thermal cycling aging, the thickness of Cu_6Sn_5 layer decreased, e.g., about 0.4 μm, for Cu_3Sn layer, about 1.6 μm, for total IMC. As mentioned above with rare earth Ce, the smaller IMC layer thickness obtained with Ce addition would be beneficial to improve the long-term reliability of SnAgCu solder joint.

In order to further investigate the effect of rare earth Ce on the properties of SnAgCu solder, the activation energy of IMC layer was calculated based on the Eqs. (3)–(5). The calculated results, activation energies for total IMC layer ($Cu_6Sn_5 + Cu_3Sn$), Cu_6Sn_5 layer and Cu_3Sn layer, are displayed in Table 1. The activation energy for the IMC growth during aging is estimated to be 73.5 kJ/mol for SnAgCu/Cu and 89.4 kJ/mol for SnAgCuCe/Cu. Consequently, the IMC growth rate is much higher for the SnAgCu/Cu system than that for the SnAgCuCe/Cu system according to the smaller activation

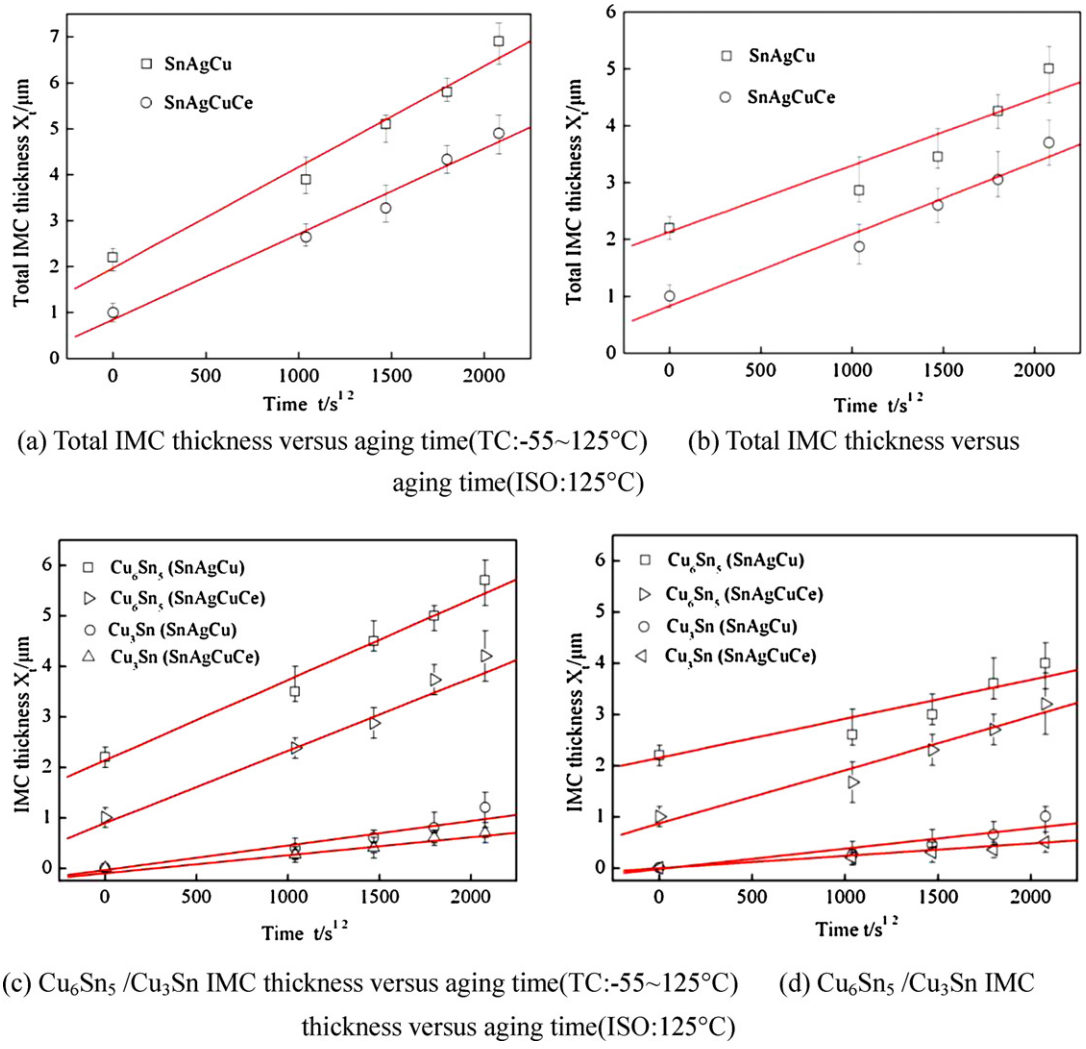

Fig. 10. IMC thickness versus aging time: (a) total IMC thickness versus aging time (TC: −55 to 125 °C), (b) total IMC thickness versus aging time (ISO: 125 °C), and (c) Cu_6Sn_5/Cu_3Sn thickness versus aging time (TC: −55 to 125 °C), and (d) Cu_6Sn_5/Cu_3Sn IMC thickness versus aging time (ISO: 125 °C).

energy for the IMC growth ($Cu_6Sn_5 + Cu_3Sn$, Cu_6Sn_5 and Cu_3Sn), especially for Cu_3Sn layer. Table 1 shows activation energies data form previous work. Although some scatter does occur in the data, it follows the Arrhenius equation. Comparing the materials and experiments, the discrepancy among the activation energies is due to the differences in the solder materials, diffusion couple methods, aging conditions (temperatures and times) and relative analytical method used. In this work, the activation energy of intermetallic compound exhibited lower than that of the previous work [55] due to a higher growth rate constant at low temperatures.

Table 1
Activation energy calculated of SAC/SACC.

Solder/substrate	Temperature range (°C)	Reaction time (days)	IMCs	Activation energy (kJ/mol)	Reference
Sn–3.8Ag–0.7Cu/Cu	100–140	0–30 days	$Cu_6Sn_5 + Cu_3Sn$	73.5	This work
	100–140	0–30 days	Cu_6Sn_5	61.4	
	100–140	0–30 days	Cu_3Sn	105.8	
Sn–3.8Ag–0.7Cu–0.03Ce/Cu	100–140	0–30 days	$Cu_6Sn_5 + Cu_3Sn$	89.4	This work
	100–140	0–30 days	Cu_6Sn_5	68.7	
	100–140	0–30 days	Cu_3Sn	119.6	
Sn–0.6Cu–0.05Ni/Cu	80–150	0–60 days	$Cu_6Sn_5 + Cu_3Sn$	76.17	[58]
	80–150	0–60 days	Cu_6Sn_5	66.35	
Sn–3.0Ag0.5Cu/Cu	100–170	0–28 days	$Cu_6Sn_5 + Cu_3Sn$	75.1	[60]
	100–170	0–28 days	Cu_6Sn_5	58.3	
	100–170	0–28 days	Cu_3Sn	114.7	
Sn–3.2Ag–0.8Cu/Cu	70–150	20–500 h	$Cu_6Sn_5 + Cu_3Sn$	70	[61]
	70–150	20–500 h	Cu_6Sn_5	72	
	70–150	20–500 h	Cu_3Sn	69	
Sn–3.8Ag–0.7Cu/Cu	125–170	0–1500 days	$Cu_6Sn_5 + Cu_3Sn$	92.6	[55]
	125–170	0–1500 days	Cu_6Sn_5	83.9	
	125–170	0–1500 days	Cu_3Sn	102	

4. Conclusions

The kinetic analysis of the growth of IMC formed between SnAgCu–*x*Ce solder ($x = 0$, 0.03 wt.%) and Cu substrate was performed during thermal cycling and isothermal aging. In the present study, thermal cycling and isothermal aging studies were performed on solder joints, to investigate the formation and growth of the intermetallic compound (IMC) at the solder (SnAgCu or SnAgCuCe)/Cu interface. In this work, morphology and growth kinetics of the formed intermetallic compounds (IMC) layer in both systems are investigated under different aging conditions. The results show that the morphology of IMCs formed both at SnAgCu/Cu and SnAgCuCe/Cu interfaces gradually changed from scallop-like to planar-like, and different IMC thickness developed with increasing aging time. Furthermore, IMC growth rate at both interfaces during thermal cycling aging was higher than that during isothermal aging. The activation energy for the IMC growth during aging is estimated to be 73.5 kJ/mol for SnAgCu/Cu and 89.4 for SnAgCuCe/Cu. Consequently, the IMC growth rate is much higher for the SnAgCu/Cu system than for the SnAgCuCe/Cu system according to the smaller activation energy for the IMC growth ($Cu_6Sn_5 + Cu_3Sn$, Cu_6Sn_5 and Cu_3Sn), especially for Cu_3Sn layer. In particular, the addition of trace Ce to the SnAgCu solder can refine the microstructures and decrease the thickness of the intermetallic compound layer of SnAgCu solder alloys.

Acknowledgments

The present work was carried out with the support of Nanjing University of Aeronautics and Astronautics Doctoral Dissertation Innovation and Excellence Producing foundation (Project No. BCXJ09-07) and the Jiangsu General Colleges and Universities Postgraduate Scientific Research Innovative Plan (Project No. CX09B-074Z).

References

[1] A.A. EI-Daly, A.E. Hammad, J. Alloys Compd. 509 (2011) 8554–8560.
[2] H.F. Zou, H.J. Yang, Z.F. Zhang, Acta Mater. 56 (2008) 2649–2662.
[3] D.G. Kim, S.B. Jung, J. Alloys Compd. 386 (2005) 151–156.
[4] A.A. EI-Daly, A. Fawzy, A.Z. Mohamad, A.E. EI-Taher, J. Alloys Compd. 509 (2011) 4574–4582.
[5] L.C. Tsao, J. Alloys Compd. 509 (2011) 8441–8448.
[6] A. Piereiková, J. Bednarcik, J. Durisin, J. Alloys Compd. 509 (2011) 1550–1553.
[7] Z.J. Han, S.B. Xue, J.X. Wang, X. Zhang, L. Zhang, S.L. Yu, H. Wang, Trans. Nonferrous. Met. Soc. China 18 (2008) 814–818.
[8] K.S. Kim, S.H. Huh, K. Suganuma, J. Alloys Compd. 352 (2003) 226–236.
[9] W.X. Dong, Y.W. Shi, Y.P. Lei, Z.D. Xia, F. Guo, J. Electron. Mater. 38 (2009) 1906–1912.
[10] L. Zhang, S.B. Xue, Y. Chen, Z.J. Han, J.X. Wang, S.L. Yu, F.Y. Lu, J. Rare Earth 27 (2009) 138–144.
[11] N. Hidaka, H. Watanale, M. Yoshiba, J. Electron. Mater. 38 (2009) 670–677.
[12] J. Zhao, C.Q. Cheng, L. Qi, C.Y. Chi, J. Alloys Compd. 473 (2009) 382–388.
[13] Y.W. Wang, Y.W. Lin, C.R. Kao, J. Alloys Compd. 478 (2009) 121–127.
[14] L.W. Lin, J.M. Song, Y.S. Lai, Y.T. Chiu, N.C. Lee, J.Y. Uan, Microelectron. Reliab. 49 (2009) 235–241.
[15] I.E. Anderson, J.C. Foley, B.A. Cook, J. Harringa, R.L. Terpstra, O. Unal, J. Electron. Mater. 30 (2001) 1050–1059.
[16] F.J. Wang, Z.S. Yu, Y.Y. Qian, J. Alloys Compd. 438 (2007) 110–115.
[17] Z.Y. Zhong, H. Saka, T.H. Kim, E.A. Holm, Y.F. Han, X.S. Xie, Mater. Sci. 47 (2005) 5–479 (2005) 1747–1750.
[18] K. Kanlayasiri, M. Mongkolwongrojn, T. Ariga, J. Alloys Compd. 485 (2009) 225–230.
[19] L. Ye, Z.H. Lai, J. Liu, A. Thölén, Solder. Surf. Mt. Technol. 13 (2001) 16–20.
[20] B.L. Chen, G.Y. Li, Thin Solid Films 462-463 (2004) 395–401.
[21] P. Yao, P. Liu, J. Liu, Microelectron. Eng. 84 (2009) 1969–1974.
[22] M.A. Dudek, R.S. Sidhu, N. Chawla, M. Renavikar, J. Electron. Mater. 35 (2006) 2088–2097.
[23] M.A. Dudek, N. Chawla, Intermetallics 18 (2010) 1016–1020.
[24] J.X. Wang, S.B. Xue, Z.J. Han, S.L. Yu, Y. Chen, Y.P. Shi, H. Wang, J. Alloys Compd. 467 (2009) 219–226.
[25] C.M.T. Law, C.M.L. Wu, D.Q. Yu, L. Wang, J.K.L. Lai, J. Electron. Mater. 35 (2006) 89–93.
[26] C.M.L. Wu, D.Q. Yu, C.M.T. Law, L. Wang, Mater. Sci. Eng. R 44 (2004) 1–44.
[27] J.F. Li, S.H. Mannan, M.P. Clode, D.C. Whalley, D.A. Hutt, Acta Mater. 54 (2006) 2907–2922.
[28] M.O. Alam, H. Lu, C. Bailey, Y.C. Chan, Comput. Mater. Sci. 45 (2009) 576–583.
[29] Y.D. Lu, X.Q. He, Y.F. En, X. Wang, Z.Q. Zhuang, Acta Mater. 57 (2009) 2560–2566.
[30] N.S. Liu, K.L. Lin, J. Alloys Compd. 456 (2008) 466–473.
[31] M. He, Z. Chen, G.J. Qi, Acta Mater. 52 (2004) 2047–2056.
[32] K.N. Tu, A.M. Gusak, M. Li, J. Appl. Phys. 93 (2003) 1335–1353.
[33] T. Laurila, V. Vuorinen, J.K. Kivilahti, Mater. Sci. Eng. R 49 (2005) 1–60.
[34] Y.C. Chan, A.C.K. So, J.K.L. Lai, Mater. Sci. Eng. B 55 (1998) 5–13.
[35] P.J. Shang, Q.Z. Liu, D.X. Li, J.K. Shang, Scripta Mater. 59 (2008) 317–320.
[36] W.Q. Peng, E. Monlevade, M.E. Marques, Microelectron. Reliab. 47 (2007) 2161–2168.
[37] K.N. Tu, R.D. Thompson, Acta Metall. 30 (1982) 947–952.
[38] H. Gan, K.N. Tu, J. Appl. Phys. 97 (2005) 063514.
[39] X. Ma, Analysis of Mechanical and Metallurgical Factors Relative to the Failure of Microelectronic Surface Mount Solder Joint, Harbin Institute of Technology, Harbin, 2000.
[40] L. Zhang, S.B. Xue,.L.L. Gao, G. Zeng, Z. Sheng, Y. Chen, S.L. Yu, J. Mater. Sci: Mater. Electron. 20 (2009) 685–694.
[41] H.T. Lee, M.H. Chen, Mater. Sci. Eng. A 333 (2002) 24–34.
[42] D.Q. Yu, J. Zhao, L. Wang, J. Alloys Compd. 376 (2004) 170–175.
[43] L. Zhang, S.B. Xue, L.L. Gao, Y. Chen, S.L. Yu, Z. Sheng, G. Zeng, J. Mater. Sci. Mater. Electron. 20 (2009) 1193–1199.
[44] J.W. Yoon, S.B. Jung, J. Mater. Sci. 39 (2004) 4211–4217.
[45] S. Ahat, M. Sheng, L. Luo, J. Electron. Mater. 30 (2001) 1317–1322.
[46] S.M.L. Nai, J. Wei, M. Gupta, J. Alloys Compd. 473 (2009) 100–106.
[47] L.H. Xu, J.H.L. Pang, K.H. Prakash, T.H. Low, IEEE Trans. Compon. Packag. Technol. 28 (2005) 408–414.
[48] J.W.R. Teo, Y.F. Sun, Acta Mater. 56 (2008) 242–249.
[49] T.Y. Lee, W.J. Choi, K.N. Tu, J.W. Jang, S.M. Kuo, J.K. Lin, D.R. Frear, K. Zeng, J.K. Kivilahti, J. Mater. Res. 17 (2) (2002) 291–301.
[50] C.K. Chung, J.G. Duh, C.R. Kao, Scripta Mater. 63 (2010) 258–260.
[51] Y.W. Wang, Y.W. Lin, C.R. Kao, J. Alloys Compd. 493 (2010) 233–239.
[52] X. Ma, F. Yoshida, Mater Lett. 56 (2002) 441–445.
[53] C.C. Pan, C.H. Yu, K.L. Lin, Appl. Phys. Lett. 93 (2008) 061912.
[54] K.N. Tu, T.Y. Lee, J.W. Jang, L. Li, D.R. Frear, K. Zeng, J.K. Kivilahti, J. Appl. Phys. 89 (2001) 4843–4849.
[55] T.Y. Lee, W.J. Choi, K.N. Tu, J.W. Jang, S.M. Kuo, J.K. Lin, D.R. Frear, K. Zeng, J.K. Kivilahti, J. Mater. Res. 17 (2002) 291–301.
[56] J. Hu, A.M. Hu, M. Li, D.L. Mao, Mater. Charact. 61 (2010) 355–361.
[57] R. Mayappan, Z.A. Ahmad, Intermetallics, doi:10.1016/j.intermet.2009.11.016.
[58] .T.A. Wu, M.H. Chen, C.H. Huang, J. Alloys Compd. 476 (2009) 436–440.
[59] J.W. Yoon, Y.H. Lee, D.G. Kim, H.B. Kang, S.J. Suh, C.W. Yang, C.B. Lee, J.M. Jung, C.S. Yoo, S.B. Jung, J. Alloys Compd. 381 (2004) 151–157.
[60] J.W. Yoon, B.I. Noh, B.K. Kim, C.C. Shur, S.B. Jung, J. Alloys Compd. 486 (1–2) (2009) 142–147.
[61] T.A. Siewert, J.C. Madeni, S. Liu, Formation and growth of intermetallics at the interface between lead-free solders and copper substrate[J]. Proceedings of the APEX Conference on Electronics Manufacturing, Anaheim, California, April, 2003. 23 (7) 583–594.